Materials Today Communications 22 (2020) 100766

Contents lists available at ScienceDirect

Materials Today Communications

journal homepage: www.elsevier.com/locate/mtcomm

Biologically synthesized copper and zinc oxide nanoparticles for important biomolecules detection and antimicrobial applications

Muthuchamy Maruthupandy[a,b,*], Thillaichidambaram Muneeswaran[b], Govindan Rajivgandhi[c], Franck Quero[b], Muthusamy Anand[d], Ji-Ming Song[a,**]

[a] School of Chemistry & Chemical Engineering, Anhui Province Key Laboratory of Chemistry for Inorganic/Organic Hybrid Functionalized Materials, Anhui University, Hefei, Anhui 230 601, PR China

[b] Laboratorio de Nanocelulosa y Biomateriales, Departamento de Ingeniería Química, Biotecnología y Materiales, Facultad de Ciencias Físicas y Matemáticas, Universidad de Chile, Avenida Beauchef 851, Santiago, Chile

[c] State Key Laboratory of Biocontrol and Guangdong Provincial Key Laboratory of Plant Resources, School of Life Sciences, Sun Yat-sen University, Guangzhou 510275, PR China

[d] Department of Marine and Coastal Studies, School of Energy, Environment and Natural Resources, Madurai Kamaraj University, Madurai 625 021, Tamil Nadu, India

ARTICLE INFO

Keywords:
CuO and ZnO NPs
Optical sensor
Biomolecules
Cysteine and NADH
Antibacterial and antifungal activity

ABSTRACT

In the present study, we report CuO and ZnO nanoparticles (NPs) synthesized through biological route using *Camellia japonica* plant leaf extract and their efficiency detection of cysteine and dihydronicotinamide adenine dinucleotide (NADH) in addition to their antimicrobial properties. Changes in absorption peak intensity in the presence of cysteine or NADH was assessed by UV–vis spectrophotometry. The spectrometric detection limit for the cysteine and NADH was found to be 5 and 10 μM, respectively, for both CuO and ZnO NPs. Good linear relationships with $R^2 = 0.9727$ for CuO and 0.9862 for ZnO NPs were obtained when plotting the absorbance as a function of cysteine and NADH concentrations at 290 and 301 nm, respectively. The present metal oxide (CuO and ZnO) NPs sensors were found to be useful for the detection of two biomolecules; namely cysteine and NADH. Furthermore, the CuO and ZnO NPs were found to be highly effective against gram positive (*Streptococcus pneumoniae*, *Bacillus subtilis*) and gram negative (*Escherichia coli*, *Salmonella typhimurium*) bacterial pathogens as well as fungal strains of *Aspergillus flavus, Aspergillus fumigates, Aspergillus niger* and *Candida albicans*. A minimum inhibition concentration of 100 μg/mL was observed for both NPs against bacterial and fungal pathogens. Consequently, the present investigation offers an environmentally friendly approach to synthesize CuO and ZnO NPs for biomolecule detection as well as antimicrobial and antifungal applications.

1. Introduction

Cysteine is an essential amino acid involved in metabolism, detoxification and protein folding. It may cause certain diseases, including Parkinson's disease and Alzheimer's disease. In addition, cysteine has been used in the food industry to flavor meat as well as in the baking industry as quality improver of biscuits and cakes and also in the personal care industry [1]. Dihydronicotinamide adenine dinucleotide (NADH) is an important coenzyme present in all living systems. It is involved in metabolic processes acting as electron carrier during respiration and photosynthesis [2]. More than 300 NADH dependent dehydrogenase enzymes that are involved in energy metabolism, growth, differentiation have been identified [3]. Sensing these NADH dependent dehydrogenases, is however, challenging and might be a promising approach in the field of pollution control, food biology, clinical and other bioprocess monitoring [4]. Numerous methods including spectrophotometric, fluorimetric, electrochemical, electrophoretic and high-performance liquid chromatographic have been proposed for the detection of cysteine and NADH. These methods are, however, expensive, time consuming with relatively low sensitivity and often high complexity. Hence, it is necessary to find alternative methods to detect these biomolecules that do not present these obstacles.

Microbial communicable diseases are sedated health difficulties it has haggard the public tending in global as a human welfare menace, which widens to worldly and societal complications. Furthermore, combating microbial pathogens with established antibiotics is under

* Corresponding author at: School of Chemistry & Chemical Engineering, Anhui Province Key Laboratory of Chemistry for Inorganic/Organic Hybrid Functionalized Materials, Anhui University, Hefei, Anhui 230 601, PR China.

** Corresponding author.

E-mail addresses: mmaruthupandy@yahoo.in (M. Muthuchamy), jiming@ahu.edu.cn (S. Ji-Ming).

https://doi.org/10.1016/j.mtcomm.2019.100766
Received 6 May 2019; Received in revised form 5 November 2019; Accepted 7 November 2019
Available online 08 November 2019

threat since most of the pathogens develop resistance to antibiotics. Soon, according to WHO, efficient therapeutics against microbial pathogens will be scarce and the universe will enter into “post antibiotic era”. Hence, there is a growing demand for treating such pathogens with novel strategy and materials.

Research on nanoparticles (NPs) has increased considerably since these particles have interdisciplinary applications in the field of physics, chemistry and biology. Metallic and non-metallic NPs with a wide range of properties and applications have been reported elsewhere [4–7]. The use of nanomaterial-based optical sensor has increased considerably for the detection of biological molecules [8–12]. The application of nanomaterials in optical sensor has been discussed extensively in literatures [13–15,7]. Optical sensors have been showing advantages of selectivity, sensitivity, accuracy, linearity, reproducibility, resolution, dynamic range, and limit of detection [9,16]. More particularly, gold and silver NPs have been studied extensively and have been shown to possess wide range of applications in biomedicine, sensors, electronics and bio-analytics [10,17,18].

Metal oxide NPs possess interesting physical and biological properties including conductivity, luminescence, absorbance and biocompatibility. They are commonly used for sensor applications [19,20]. ZnO and CuO are p-type and n-type semiconductor materials, respectively, with a constrictive band gap of 1.7 eV and 3.34 eV at room temperature [21]. In addition to Au and Ag NPs, ZnO and CuO metal oxide NPs have been utilized as colorimetric sensors alone or in composite materials. According to Acres et al. [22], sulfide anions that are present in the molecular structure of cysteine, cause color change of Cu@AuNPs colloidal suspensions from purple to red. Furthermore, a visible color change for synthesized CuO/ZnO nanocomposites has been observed to the naked eye for cysteine [23].

It has been shown that size, shape, morphology, ligand type and method of synthesis influence the applicability of these NPs and vast literature is available for their controlled synthesis [24,25]. Cu NPs, however, can be easily oxidized when exposed to air or aqueous medium. As a result, the synthesis of stable Cu NPs is particularly challenging. Copper NPs possess similar surface plasmon resonance (SPR) properties to gold and silver NPs and are comparably cheaper. As a result, copper NPs could be a potential and promising alternative to gold and silver NPs. In addition, copper NPs have been applied in various fields [26–28] but their application for colorimetric application of Cu NPs is scarce. To date, to the best of our knowledge, this is the first report on the detection of cysteine and NADH that is based on an optical sensing method using CuO and ZnO NPs. Various chemical and biological methods have been proposed for the synthesis of CuO and ZnO NPs. Green synthesis of NPs via biological routes is of great interest since these present several advantages over chemical methods, including the use of natural products. Very few reports, however, have reported the use of plant-extract-mediated synthesis of CuO and ZnO NPs [29,30].

In the present study, biologically (*C. japonica*) synthesized CuO and ZnO NPs were used to optically detect l-cysteine as well as NADH. The synthesis and more detailed characterization of these NPs has been reported in our previous publication by Maruthupandy et al., [26]. Furthermore, in the present study, CuO and ZnO NPs were tested for their antimicrobial activity against gram positive bacteria (GPB); namely *S. pneumoniae* and *B. subtilis* as well as gram negative bacteria (GNB); namely *E. coli* and *S. typhimurium*) as well as *A. flavus, A. fumigates, A. niger* and *C. albicans* fungal strains.

2. Materials and methods

2.1. Materials and chemicals

Cysteine and NADH were purchased from Aladdin chemicals, China. Stock solutions for each biomolecule type were prepared by dissolving a known weight in a known volume of deionized water. All the glassware was thoroughly washed with deionized water prior to use. The bacterial and fungal strains were collected from the Bose laboratory, Kalavasal, Madurai, Tamil Nadu India. Sterile discs were purchased from Himedia chemicals Pvt. Ltd., India and subsequently used for antibacterial and antifungal activity evaluation.

2.2. Biological synthesis and characterization of CuO and ZnO NPs

2.2.1. Synthesis of CuO NPs

The CuO NPs synthesis was carried out by following the modified approach of Sharma et al., [24]. Brielfy, 100 mL of *C. japonica* leaf extract was heated up to 60–80 °C using an oil bath under stirring. ~10 g of cuprous nitrate (Cu $(NO_3)_2.3H_2O$) was subsequently dissolved in the leaf extract under constant stirring in an oil bath. After complete dissolution, the mixture was boiled until forming a black colored paste. The paste was recovered in a ceramic crucible and heated in an air-heated furnace at 400 °C for 2 h to finally obtain CuO NPs.

2.2.2. Synthesis of ZnO NPs

ZnO NPs were synthesized by following the modified method of Elumalai et al., [27]. Briefly, 100 mL of *C. japonica* leaf aqueous extract was taken from the stock solution and heated at 60–80 °C using an oil bath. When the temperature of the solution reached 60 °C, ~10 g of zinc nitrate hexahydrate ($Zn(NO_3)2{\cdot}6H_2O$) was added. The mixture was allowed to boil until obtaining a yellow colored paste. Then, the past was recovered into a ceramic crucible cup and heated up in an air-heated furnace for 3 h at 400 °C. A light yellowish/whitish colored powder (ZnO NPs) was obtained, which was used for the subsequent studies.

2.2.3. Characterization of CuO NPs

The synthesized CuO and ZnO NPs were characterized at room temperature by UV–vis spectroscopy (UV–vis spectrophotometer, Shimadzu, UV-1750) and Fourier-transform infrared (FTIR) spectroscopy (Nicolet NEXUS-870). FTIR spectra were recorded in the range of $4000-400\ cm^{-1}$. Powder X-ray diffraction (XRD) measurements were performed using a Rigaku D/max-RA X-ray diffractometer equipped with Cu-Kα radiation having a wavelength of 1.54178 Å. The morphology, size and composition of CuO and ZnO NPs were assessed by scanning electron microscopy (SEM, Hitachi S-4800) coupled with energy-dispersive X-ray spectroscopy (EDS) and by transmission electron microscopy (TEM, Hitachi JEM-2100).

2.3. Optical sensor of biomolecules

The synthesized CuO and ZnO NPs were used as optical sensors for cysteine and NADH (Scheme 1). An aqueous solution of cysteine and NADH were added, individually, to the CuO and ZnO NPs solution with a corresponding absorbance value of ~1 (Scheme 2). The changes observed in the optical absorption band of CuO and ZnO NPs due to the presence of both biomolecule types were monitored by UV–vis spectrophotometry.

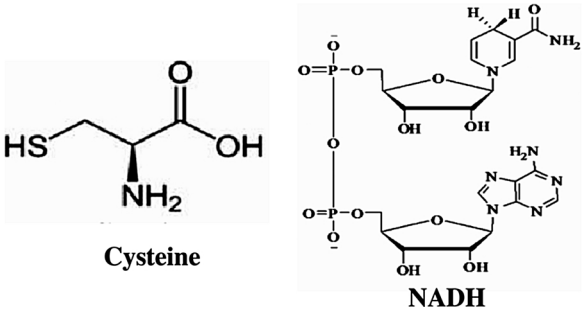

Scheme 1. Molecular structures of cysteine and NADH.

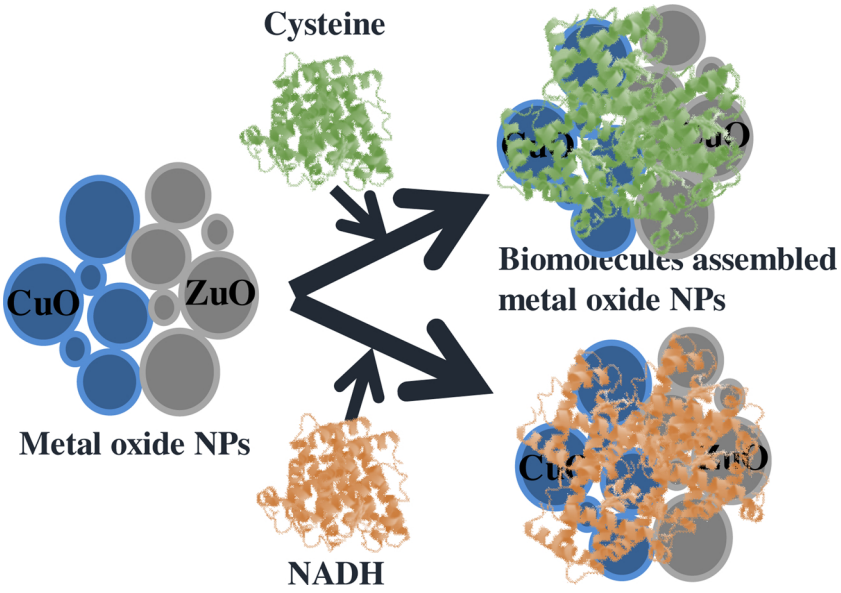

Scheme 2. Biomolecules interaction with metal oxide NPs.

2.4. Antimicrobial studies

The antibacterial activity of CuO and ZnO NPs was carried out against GPB (*B. subtilis* and *S. pneumoniae*) and GNB (*E. coli* and *S. typhimurium*) by using the agar disc diffusion method. Sterile discs of 6 mm diameter were placed into Mueller Hinton agar (MHA) medium containing the test microorganism. The discs were filled with 40 µL of CuO and ZnO NPs separately at concentrations of 20, 40, 60, 80, 100 µg/mL. Streptomycin was used as positive control and DMSO solution without NPs acted as negative control. The plates were incubated for 18 h at 37 °C.

The antifungal activity of CuO and ZnO NPs was assessed against four fungal strains (*A. flavus, A. fumigates, A. niger* and *C albicans*) using the agar disc diffusion method. Sterile discs of 6 mm diameter were placed into the potato dextrose agar (PDA) medium that contained the test microorganism. The discs were filled with 40 µL of CuO and ZnO NPs at concentrations of 20, 40, 60, 80, 100 µg/mL and placed on the MHA plates, separately. Amphotericin-B was used as positive control and DMSO solution without NPs as negative control. The plates were incubated for four days at 25 °C. Antibacterial and antifungal activity was evaluated by measuring the inhibition zone towards each microorganism being tested.

3. Result and discussion

3.1. Characterization of CuO and ZnO NPs

The UV–vis absorption spectrum curves of the mono dispersed CuO and ZnO NPs are reported in Fig. S1a-c. The spectra exhibit strong absorption peaks at wavelength positions of ~290 nm for CuO NPs and of ~301 nm for ZnO NPs. The periodical observation of the synthesized CuO and ZnO NPs using UV–vis spectral analysis suggests that no significant change in the morphology, position and symmetry of the absorption peak height even after 30 days may have occurred (Fig. S1a,b). This indicates that the synthesized CuO and ZnO NPs are highly stable [31]. The photoluminescence (PL) spectra of the CuO and ZnO NPs are displayed in Fig. S2a. FTIR spectra and powder XRD patterns corresponding to biologically synthesized CuO and ZnO NPs using *C. japonica* leaf extract are reported in Fig. S2b and Fig. S2c, respectively. Narrow and strong diffraction peak of CuO and ZnO NPs indicate that the products are highly crystalline in nature. SEM images show that the obtained CuO (Fig. S3a,b) and ZnO NPs (Fig. S4a,b) possess spherical shape and are well distributed forming aggregates. TEM analysis of CuO and ZnO NPs show the formation of monodispersed and spherical nanoparticles with a small size distribution in the range ~15 – 25 nm with an average size value of ~17 nm (Fig. S3 c,d) and ~15 – 30 nm with an average size of ~20 nm (Fig. S4 c,d), respectively. Little attention has been paid to how synthesis process is influenced by the agglomeration state of NPs. The ability of NPs to agglomerate is, however, one of the predominant problems associated to NPs suspensions. Changes in pH and ionic strength or the presence of biomolecules, particularly proteins, can easily modify the NPs surface properties, leading to the loss of colloidal stability and formation of agglomerates [32].

3.2. Optical sensor of biomolecules

3.2.1. Cysteine

The absorption spectral changes observed for CuO and ZnO NPs upon the addition of 5 µM cysteine is illustrated in Fig. 1a, c. The absorption spectrum acquired for CuO and ZnO NPs show a characteristic absorption peak at wavelength positions of ~290 and 301 nm, respectively [33]. Figs. 1a (b–f), 1c (b–f)) indicate a significant decrease in the absorption band intensity of CuO and ZnO NPs upon the addition of each 5 µM cysteine. Due to the binding of cysteine with CuO NPs, the isosbestic point was observed at a wavelength position of ~317 nm [34]. This decrease in the absorption intensity of CuO NPs may attribute to the cysteine induced CuO NPs assembly [35]. It has been shown that cysteine can easily attached onto the surface of both NPs. Additionally, the interaction between cysteine and NPs has been reported to be partially electrostatic and also partially covalent [36]. Previous results suggested that decrease in intensity of the absorption peak of CuO and ZnO NPs can occur due to aggregation of NPs [37].

Shifts in the absorption peak of CuO and ZnO NPs towards lower wavelength positions depends on the concentration of cysteine in the solution. Fig. 1b, d. shows the corresponding calibration plot of absorbance ($A_{290\ nm}$ and $A_{301\ nm}$) changes during the addition of cysteine. The calibration curve shows a good linear relationship (R^2 = 0.9773 for CuO NPs and R^2 = 0.9693 for ZnO NPs) in the range of 5–25 µM of cysteine (Fig. 1b, d). Moreover, experimental detection limits (LOD) for both CuO and ZnO NPs was found to be 5 µM. These results may be potentially useful for the selective sensing of cysteine among other amino acids, making metal oxide (CuO and ZnO) NPs versatile for sensing biologically significant molecules.

3.2.2. Dihydronicotinamide adenine dinucleotide (NADH)

The absorption spectra recorded for CuO and ZnO NPs in the presence and absence of NADH are depicted in Fig. 2a, c. A significant

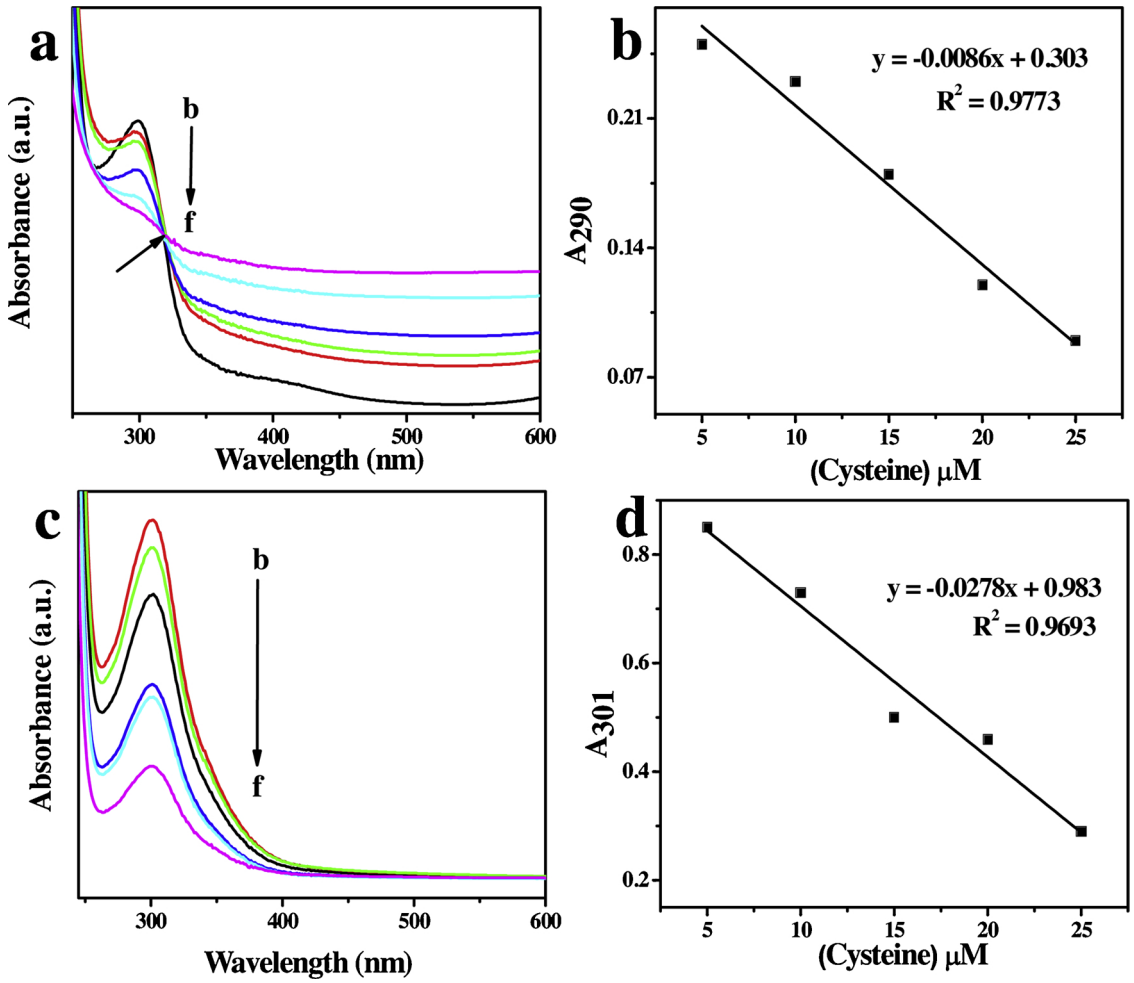

Fig. 1. UV–vis absorption spectrum of CuO NPs solution upon each addition of 5 μM of cysteine and corresponding calibration plot of CuO NPs as a function of cysteine concentration (a and b). UV–vis absorption spectrum of ZnO NPs solution upon each addition of 5 μM of cysteine and corresponding calibration plot of ZnO NPs as a function of cysteine concentration (c and d).

decrease in the intensity of the absorption peak for both NPs is observed upon adding 10 μM NADH (Fig. 2a, c). This change in absorption intensity is due to the adsorption of NADH molecules onto the surface of NPs. The attachment of NADH onto the surface of the NPs can be expected based on the nature of binding between the NPs and NADH molecules [38,10]. The optical absorption intensity of the CuO and ZnO NPs decreased significantly upon each addition of NADH (Fig. 2a, c). Due to the binding of NADH with CuO NPs, the isosbestic point was observed at a wavelength position of ~320 nm. The reduction in intensity of the peak absorption of NPs is attributed to the formation of NADH metal oxide NPs assemblies. Upon the addition of NADH, a decrease in the intensity of the peak absorption of these metal oxide NPs was observed. It has been proposed that the electronic interaction between the adsorbate and the NPs surface resulted in changes in electron density onto metal oxide NPs, leading to the decrease in the intensity of the peak absorption of metal oxide NPs. Furthermore, this results in the modification in the electronic existence of the outside band [39]. Similarly, the observation of the decrease in the intensity of the peak absorption of CuO and ZnO NPs is due to these interactions upon the addition of biomolecules. The particle size of the metal oxide NPs is also reduced due to the interaction of NADH with metal oxide. Moreover, chemisorption of NADH onto the metal oxide NPs has been found to lead to demetalization of surface copper and zinc atoms [40,41].

The NADH molecules were adsorbed onto the metal oxide NPs surface and can efficaciously bring closer together the NPs. The calibration plot presented in Fig. 2b, d reveals a linear relationship between the NADH concentration and the absorption of the metal oxide NPs. Moreover, the experimental level of detection (LOD) for both NPs was found to be 10 μM for NADH. A good linear relationship (R^2 = 0.9727 for CuO and R^2 = 0.9862 for ZnO NPs) between the absorbance and the NADH concentration at wavelength positions of ~290 and ~301 nm was obtained in the range of 10–50 μM (Fig. 2b, d). The present metal oxide (CuO and ZnO) NPs based sensor can be used for the detection of two biomolecules namely NADH and cysteine. It is interesting to note that the present metal oxide NPs are relatively simple to prepare for subsequent use as an optical sensor for the detection of these biomolecules.

Table 1 summarizes the comparative study of analytical performance of the present study with some of the previously reported optical sensor studies towards the detection of biological molecules. The present work is the first study to report CuO and ZnO NPs based optical biosensor for the detection of NADH and cysteine. Numerous reports are, however, available on the use of other metal (silver/gold) NPs as optical sensors. Tseng and co-workers [42] reported that functionalized Au NPs support detection of 1 μM cysteine (with linearity in the range of 5–500 μM). Mirkin and co-workers [43] reported the detection of 50 nM cysteine (with linearity in the range of 50 nM-10 μM) using DNA–gold NPs based sensor. Wei et al. [44] demonstrated that carboxymethyl cellulose mediated Au NPs can be used as optical biosensor for the detection of 10 μM cysteine (with linearity in the range of 10–100 μM). Willner and coworkers [45] showed that ~100 μM NADH can be detected utilizing adapted Au NPs (with linearity in the limit of 100 μM–10 mM). The two metal oxide NPs synthesized in the present

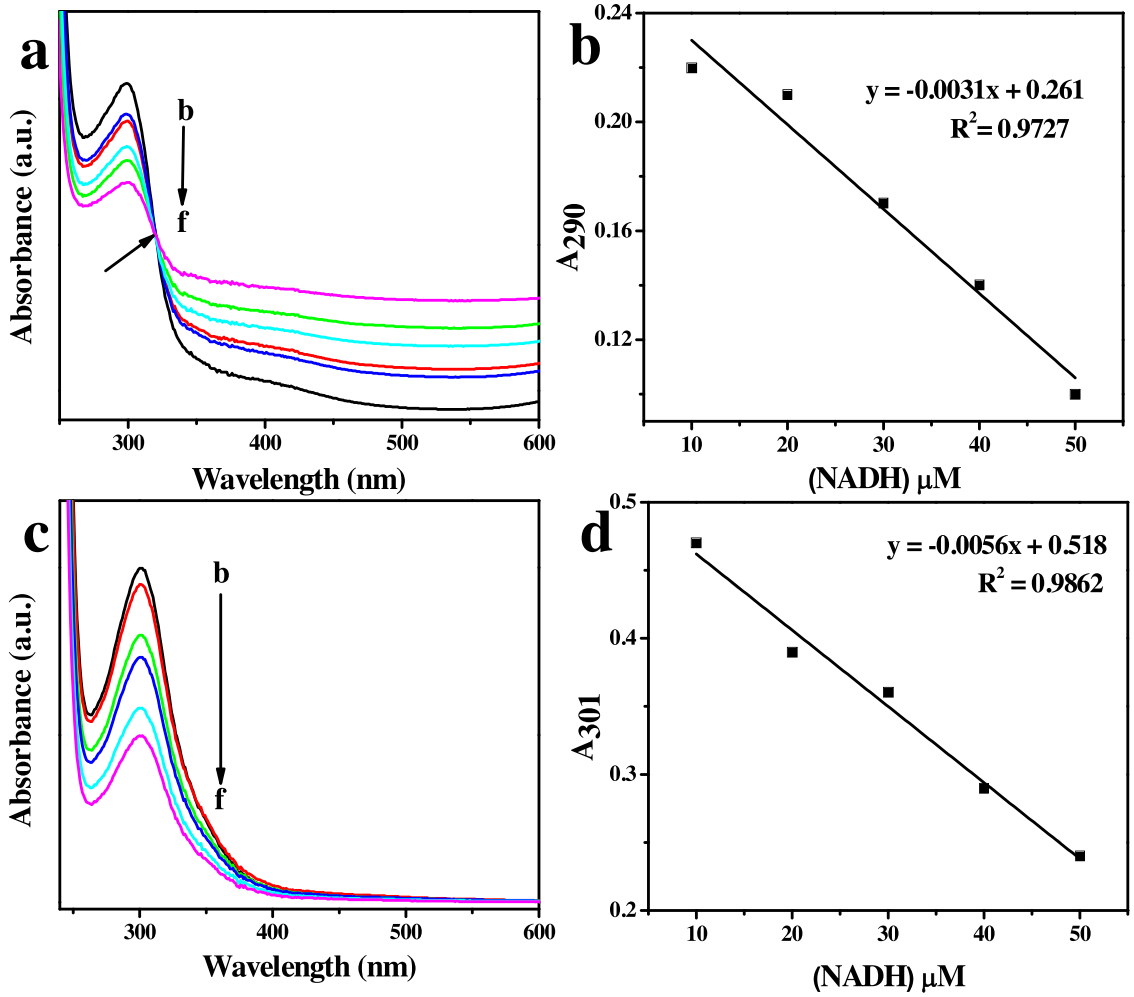

Fig. 2. UV–vis absorption spectrum of CuO NPs solution upon addition of he each addition of 5 µM NADH and corresponding calibration plot of CuO NPs as a function of NADH concentration (a and b). UV–vis absorption spectrum of ZnO NPs solution upon each addition of 5 µM of NADH and corresponding calibration plot of ZnO NPs as a function of NADH concentration (c and d).

study support the detection of NADH and cysteine at lower detection limits (5 and 10 µM concentrations, respectively).

3.3. Antibacterial and antifungal activity of CuO and ZnO NPs

3.3.1. Antibacterial activity

The antibacterial activity of CuO and ZnO NPs against GPB were found to be 9, 21 mm and 11, 11.5 mm for *S. pneumoniae* and *B. subtilis* at 100 µg/mL concentration, respectively. The NPs showed better activity against GNB with zone of inhibition 10.5, 18 mm and 11, 12 mm for *E. coli* and *S. typhimurium* (Fig. 3a,b) at 100 µg/mL concentration, respectively. The size of inhibition zone was found to increase upon increasing the concentration of CuO and ZnO NPs above 20 − 100 µg/mL (Fig. 3a, b) for all the tested bacteria. It is noteworthy that the sensitivity of *S. pneumoniae* was higher at the lowest concentration of ZnO NPs when compared to CuO NPs. On the other hand, the sensitivity of *S. pneumoniae* (21 mm) was higher at the highest concentration of ZnO NPs with maximum zone of inhibition when compared to other bacterial pathogens. Surprisingly, ZnO NPs showed better antibacterial activity than CuO NPs against all the GPB and GNB bacterial strains. Moreover, the CuO NPs showed low antibacterial effect against all the tested bacterial strains. Streptomycin (standard antibiotic disc) was

Table 1
Comparison of some reported assays with metal and metal oxide NPs for optical determination of important biomolecules including cysteine and NADH.

Materials	Analyte(s)	Analytical performance	References
Gold NPs	Cysteine	5 µM–500 µM	[34]
DNA mediated gold NPs	Cysteine	50 nM–10 µM	[35]
Carboxymethyl cellulose functionalized gold NPs	Cysteine	10 µM–100 µM	[36]
Gold NPs	NADH	100 µM–10 mM	[37]
Silver NPs	Cysteine, Adenosine NADH	5 µM–35 µM 20 µM–140 µM 5 µM–35 µM	[10]
Gold NPs	Adenosine	30 µM–200 µM	[55]
Gold NPs	Glucose	10 µM–400 µM	[56]
DNA mediated gold NPs	Oligonucleotide	50 pM–5 nM	[57]
Gold NPs	Adrenaline	5 µM–200 µM	[58]
Biologically synthesis copper and zinc oxide NPs	Cysteine	5 µM– 25 µM	Present work
Biologically synthesis copper and zinc oxide NPs	NADH	10 µM–50 µM	

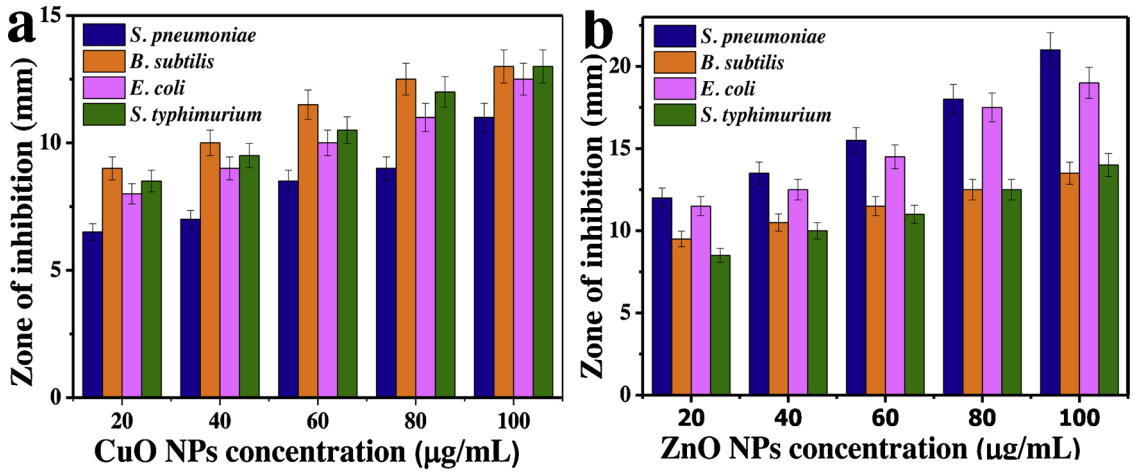

Fig. 3. Zone of inhibition of biologically synthesized CuO and ZnO NPs with different concentrations against respective bacterial pathogens.

Table 2
Antibacterial activity of CuO and ZnO NPs.

Bacterial strains	Zone of inhibition (mm)			
	CuO NPs (100 µg/mL)	ZnO NPs (100 µg/mL)	Positive control (Streptomycin)	Negative control (DMSO)
S. pneumoniae	11	21	14	–
B. subtilis	13	13.5	19.5	–
E. coli	12.5	19	21	–
S. typhimurium	13	14	20	–

used as positive control, and DMSO was used as negative control. The observed zone of inhibition for streptomycin was 12, 19.5, 19 and 20 mm for the respective bacterial strains (Table 2). DMSO did not show any zone of inhibition against all the tested pathogens. Although CuO and ZnO NPs exhibited enhanced antibacterial activity at lower concentrations, i.e. above 20 µg/mL (Fig. 3a, b), the dose of 100 µg/mL was found to be more effective in inhibiting bacterial growth (Fig. S5).

A previous report of Abboud et al. [46], showed that biologically synthesized CuO NPs interfere in the bacterial regeneration and inhibit the growth of *E. aerogenes* and *S. aureus* (21 and 15 mm) at concentrations higher than 20 µL. Similarly, Azam at al. [47] demonstrated that CuO NPs altered the multiplication of *B. subtilis* and *E. coli* at a concentration of 100 µL. Flower shaped CuO nanostructure enhanced the bacterial damage against 12 h cultures of *B. subtilis, S. paratyphi* and *E. coli* at lower concentration [48]. The increased concentration of ZnO NPs resulted in a decrease in bacterial multiplication and increased pathogenic effect against *B. subtilis and E. coli* [49]. Furthermore, it was shown that the antibacterial effect of ZnO NPs is size dependent and the damage of efflux pump and membrane is partially concentration and size dependent [50]. In our study, the synthesized ZnO NPs and CuO NPs showed better activity against GPB and two GNB. Among the four strains, *E. coli* showed greater sensitivity to ZnO NPs compared to CuO NPs, which is contradictory to the results of Chang et al. [51]. In addition, the results of Raghupathi et al. [52] depicted that ZnO NPs have significantly higher growth inhibition against *S. aureus* than biosynthesized six metal oxide NPs (MgO, TiO_2, CuO, CaO, CeO_2, and ZnO). Hence, our finding is in good agreement with some previous reports, showing that ZnO NP possess highly efficient in inhibiting some GPB and GNB.

In the present study, a difference was observed when comparing the antibacterial effect between the CuO and ZnO NPs against GPB and GNB pathogens with differed zone of inhibition. The difference in activity could be attributed to variations in the cell wall structure, cell physiology, metabolism or degree of contact. The cell wall of GNB is composed of thin layer of peptidoglycan, whereas GPB is made of a thick layer of peptidoglycan, consisting of linear polysaccharide chains crosslinked by short peptides. These GPB strains have more rigid cell wall morphology, which could difficult penetration of NPs, resulting in low antibacterial response [53,54]. Furthermore, previous studies have shown that the greater the band gap energy (ZnO NPs = 3.37 eV), the greater the efficiency in inhibiting bacterial growth, and that the effect was mediated by reactive oxygen species (ROS) [55]. In the present investigation, the antibacterial activity of ZnO NPs was found to be more efficient when compared with CuO NPs. This effect may be based on the NPs band gap energy and ROS accumulation.

3.3.2. Antifungal activity

The antifungal activity evaluation suggested that the biosynthesized CuO and ZnO NPs acted as good antifungal agents against *A. flavus, A. fumigatus, A. niger* and *C. albicans* with respective zone of inhibition of 9, 21, 11 and 11.5 mm at 100 µg/mL concentration (Table 3). The observed antifungal activity was dose dependent and the zone of inhibition increased upon increasing the concentration of CuO and ZnO NPs above 20 – 100 µg/mL (Fig. 4 a,b). Interestingly, the zone of inhibition was very high against *C. albicans* at higher concentration (80 µg/mL) when compared to other fungal pathogens (Fig. 4a, b). CuO NPs showed higher activity against *A. niger* and *C. albicans* at lower concentrations when compared to ZnO NPs. The maximum zone of inhibition observed against *A. niger* and *C. albicans* were 14 and 27 mm for CuO NPs at a concentration of 100 µg/mL. The positive control amphotericin-B (standard antibiotic) generated zones of inhibition of 12, 19.5, 19 and 20 mm against *A. flavus, A. fumigatus, A. niger* and *C. albicans* fungal strains, respectively (Table 3). The negative control did not show any zone of inhibition. The dose of 100 µg/mL was found to be highly effective for inhibiting fungal growth (Fig. S6).

Our results are in agreement with earlier finding of Ramyadevi et al. [56] who reported zones of inhibition of 13, 16, and 23 mm against *A. falvus, A. niger* and *C. albicans,* respectively for ZnO NPs. As previously documented, flower shaped CuO nanostructure exhibited zones of

Table 3
Antifungal activity of CuO and ZnO NPs.

Fungal strains	Zone of inhibition (mm)			
	CuO NPs (100 µg/mL)	ZnO NPs (100 µg/mL)	Positive control (Amphotericin-B)	Negative control (DMSO)
A. flavus	13.6	9.6	14.5	–
A. fumigatus	13.5	10.5	16	–
A. niger	24	13	14	–
C. albicans	27	19.1	12.5	–

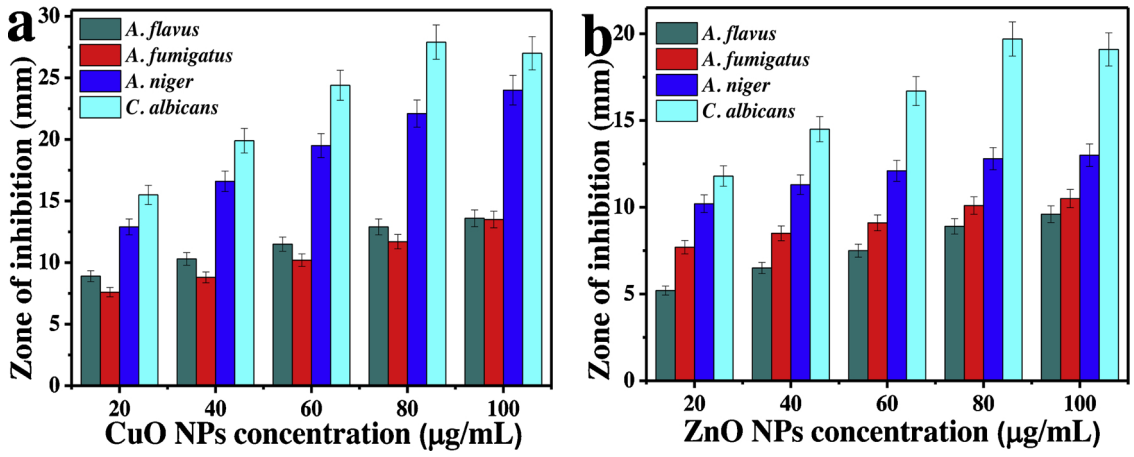

Fig. 4. Zone of inhibition of biologically synthesized CuO and ZnO NPs with different concentrations against respective fungal pathogens.

inhibition of 20 and 24 mm against *A. flavus* and *A. niger,* respectively [57]. The supportive evidence of the antifungal activity of CuO NPs exhibited that the zone of inhibition 19 and 21 mm against *A. niger* and *C. albicans.* The ZnO NPs synthesized using *Azadirachta indic*a leaf extract showed good antifungal activity with a zone of inhibition of 14.3 mm against *C. albicans* [50]. Similarly, Rajiv et al. [58] also noticed the dose dependence of the antifungal effect of plant leaf mediated synthesized ZnO NPs against plant fungal pathogens. Furthermore, the highest zone of inhibition was observed against *A. flavus* (24.6 mm) and the lowest zone of inhibition was observed against *F. culmorum* (14 mm) with ZnO NPs [59]. Previous studies have shown that the higher the band gap energy of the ZnO NPs (3.37 eV), the greater the efficiency in inhibiting the fungal growth, involving both the production of ROS and the accumulation of NPs [60–62]. In the present investigation, the antifungal activity of ZnO NPs was more efficient to compare with CuO NPs. this effect may be based on the NPs band gap energy and ROS accumulation.

With respect to the antimicrobial activity evaluation, the probable mechanism of can be attributed to disruption of cell membrane due to the release of copper ions from CuO NPs and zinc ions from ZnO NPs, which attached to the negatively charged microbial cell wall and rupture it, thereby causing protein denaturation and cell death. Once entered into microbial cell, it may bind to deoxyribonucleic acid molecules and involved in crosslinking of nucleic acid strands, forming a disorganized helical structure [63,59]. In addition, copper and zinc ions were uptaken by the microbial cells may also disturb important biochemical processes [64].

4. Conclusion

CuO and ZnO NPs optical sensing system could potentially selectively distinguish the cysteine and NADH from other analytes under similar trials. The LOD (limits of detection) of the metal oxide (CuO and ZnO) NPs optical sensors were found to be 5 and 10 µM for cysteine and NADH, respectively. To the best of our knowledge, the metal oxide (CuO and ZnO) NPs were, up to now, not used for the detection of these biomolecules. The sensing potential of CuO and ZnO NPs could be used for sensing important biological molecules (cysteine and NADH) for optical sensing devices applications. On the other hand, this study showed that CuO and ZnO NPs are promising antimicrobial agent against bacterial and fungal pathogens. The antibacterial test suggested that both gram positive (*B. subtilis* and *S. pneumoniae*) and gram negative (*P. aeruginosa* and *S. typhimurium*) bacterial strains are more prone to ZnO NPs than CuO NPs. Before commercialization, detailed research and comparative study of strain-specific variability is required to determine the bactericidal and fungicidal efficiency of these metal oxide NPs.

Declaration of competing interest

The authors declare that they have no conflict of interest.

Acknowledgment

The work was supported by the National Science Foundation of China (NSFC) (Grants 21641007, 21471001), Natural Science Foundation of Anhui Province (Grant no.1508085MB22), and Major Project of Education Department of Anhui Province (KJ2016SD63). We also thank the Key Laboratory of Environment Friendly Polymer Materials of Anhui Province, and the Postdoctoral Program, Anhui University, Hefei, Anhui Province, China. The authors are grateful to the Bose laboratory, Kalavasal, Madurai, Tamil Nadu India for the bacterial and fungal strains.

Appendix A. Supplementary data

Supplementary material related to this article can be found, in the online version, at doi:https://doi.org/10.1016/j.mtcomm.2019.100766.

References

[1] A.O. Obadina, O.B. Oyewole, G. Olaniyi, Effect of baking improvers on the quality of whole cassava biscuits, J. Food Sci. Technol. 51 (2014) 2803–2808.
[2] C. Cantó, K. Menzies, J. Auwerx, NAD+ metabolism and the control of energy homeostasis – a balancing act between mitochondria and the nucleus, Cell Metab. 22 (2015) 31–53.
[3] C. Quijano, M. Trujillo, L. Castro, A. Trostchansky, Interplay between oxidant species and energy metabolism, Redox Biol. 8 (2016) 28–42.
[4] R. Kourist, P. Domínguez de María, K. Miyamoto, Biocatalytic strategies for the asymmetric synthesis of profens – recent trends and developments, Green Chem. 13 (2011) 2607–2618.
[5] P.P.N. Vijay Kumar, U. Shameem, P. Kollu, R.L. Kalyani, S.V.N. Pammi, Green synthesis of copper oxide nanoparticles using Aloe vera leaf extract and its antibacterial activity against fish bacterial pathogens, BioNanoScience 5 (2015) 135–139.
[6] R.L. Kalyani, S.V.N. Pammi, P.P.N. Vijay Kumar, P.V. Swamy, P.K.V. Ramana Murthy, Antibiotic potentiation and anti-cancer competence through bio-mediated ZnO nanoparticles, Mater. Sci. Eng. C. 103 (2019) 109756.
[7] L.K. Ruddaraju, S.V.N. Pammi, G.S. Guntuku, V.S. Padavala, V.R.M. Kolapalli, A review on anti-bacterials to combat resistance: From ancient era of plants and metals to present and future perspectives of green nano technological combinations, Asian J. Pharm. Sci. (2019), https://doi.org/10.1016/j.ajps.2019.03.002 (In Press).
[8] E. Rauwel, L. Simón-Gracia, M. Guha, P. Rauwel, S. Kuunal, D. Wragg, Silver metal nanoparticles study for biomedical and green house applications, IOP Conf. Ser.: Mater. Sci. Eng. 175 (2017) 012011.
[9] K. Farhadi, M. Forough, R. Molaei, S. Hajizadeh, A. Ralipour, Highly selective Hg^{2+} colorimetric sensor using green synthesized and unmodified silver nanoparticles, Sens. Actuators B Chem. 161 (2011) 880–885.
[10] G. Maduraiveeran, R. Ramaraj, Silver nanoparticles embedded in amine-functionalized silicate sol–gel network assembly for sensing cysteine, adenosine and NADH, J. Nanopart. Res. 13 (2011) 4267–4276.
[11] M. Šimšíková, J. Čechal, A. Zorkovská, M. Antalík, T. Šikola, Preparation of CuO/ZnO nanocomposite and its application as a cysteine/homocysteine colorimetric and fluorescence detector, Colloids Surf. B Biointerfaces 123 (2014) 951–958.

[12] T. Mocan, C.T. Matea, T. Pop, O. Mosteanu, A.D. Buzoianu, C. Puia, C. Iancu, Development of nanoparticle-based optical sensors for pathogenic bacterial detection, Int. J. Nanobiotechnol. Pharm. 15 (2017) 25, https://doi.org/10.1186/s12951-017-0260-y.

[13] S. Chaudhary, S.K. Mehta, Selenium nanomaterials: applications in electronics, catalysis and sensors, J. Nanosci. Nanotechnol. 14 (2014) 1658–1674.

[14] N. Ullah, M. Manshaa, I. Khan, A. Qurashia, Nanomaterial-based optical chemical sensors for the detection of heavy metals in water: recent advances and challenges, Trends Analyt. Chem. 100 (2018) 155–166, https://doi.org/10.1016/j.trac.2018.01.002.

[15] X.-F. Zhang, Z.-G. Liu, W. Shen, S. Gurunathan, Silver nanoparticles: synthesis, characterization, properties, applications, and therapeutic approaches, Int. J. Mol. Sci. 17 (2016) E1534, https://doi.org/10.3390/ijms17091534.

[16] M.R. Bindhu, M. Umadevi, Silver and gold nanoparticles for sensor and antibacterial applications, Spectrochim. Acta A Mol. Biomol. Spectrosc 128 (2014) 37–45.

[17] C. Balalakshmi, K. Gopinath, M. Govindarajan, R. Lokesh, A. Arumugam, N.S. Alharbi, S. Kadaikunnan, J.M. Khaled, G. Benelli, Green synthesis of gold nanoparticles using a cheap Sphaeranthus indicus extract: Impact on plant cells and the aquatic crustacean*Artemia nauplii*, J. Photochem. Photobiol. B 173 (2017) 598–605.

[18] C.E. Rowland, C.W. BrownIII, J.B. Delehanty, I.L. Medintz, Nanomaterial-based sensors for the detection of biological threat agents, Mater. Today 19 (2016) 464–477.

[19] M.M. Rahman, M.M. Alam, A.M. Asiri, M.A. Islam, Ethanol sensor development based on ternary-doped metal oxides (CdO/ZnO/Yb2O3) nanosheets for environmental safety, RSC Adv. 7 (2017) 22627–22639.

[20] M. Nagajothi, K.T. Parthiban, S.U. Kanna, L. Karthiba, D. Saravanakumar, Fungal microbes associated with Agarwood formation, Am. J. Plant Sci. 7 (2016) 1445–1452.

[21] S. Lany, Semiconducting transition metal oxides, J. Phys. Condens. Matter 27 (2018) 283203.

[22] R.G. Acres, V. Feyer, N. Tsud, E. Carlino, K.C. Princ, Mechanisms of aggregation of cysteine functionalized gold nanoparticles, J. Phys. Chem. C 118 (2014) 10481–10487.

[23] S. Srivastava, D. Li, N. Edwards, A.M. Hynes, K. Wood, M. Al-Hamed, A.C. Wroe, D. Reaich, S.H. Moochhala, P.A. Welling, J.A. Sayer, Identification of compound heterozygous KCNJ1 mutations (encoding ROMK) in a kindred with Bartter"s syndrome and a functional analysis of their pathogenicity, Physiol. Rep. 1 (2013) e00160.

[24] J.K. Sharma, P. Srivastava, G. Singh, M.S. Akhtar, S. Ameen, Catalytic thermal decomposition of ammonium perchlorate and combustion of composite solid propellants over green synthesized CuO nanoparticles, Thermochim. Acta 614 (2015) 110–115.

[25] K.S. Khashan, G.M. Sulaiman, F.A. Abdulameer, Synthesis and antibacterial activity of cuo nanoparticles suspension induced by laser ablation in liquid, Arabian J. Sci. Eng. 41 (2016) 301–310.

[26] M. Maruthupandy, Y. Zuo, J.-S. Chen, J.-M. Song, H.-L. Niu, C.-J. Mao, S.-Y. Zhang, Y.-H. Shen, Synthesis of metal oxide nanoparticles (CuO and ZnO NPs) via biological template and their optical sensor applications, Appl. Surf. Sci. 397 (2017) 167–174.

[27] K. Elumalai, S. Velmurugan, Green synthesis, characterization and antimicrobial activities of zinc oxide nanoparticles from the leaf extract of *Azadirachta indica* (L.), Appl. Surf. Sci. 345 (2015) 329–336.

[28] P.C. Nagajyothi, P. Muthuraman, T.V.M. Sreekanth, D.H. Kim, J. Shima, Green synthesis: In-vitro anticancer activity of copper oxide nanoparticles against human cervical carcinoma cells, Arab. J. Chem. 10 (2017) 215–225.

[29] S. Saif, A. Tahir, T. Asim, Y. Chen, Plant mediated green synthesis of cuo nanoparticles: comparison of toxicity of engineered and plant mediated CuO nanoparticles towards Daphnia magna, Nanomaterials (Basel) 6 (2016) E205, https://doi.org/10.3390/nano6110205.

[30] M. Sundrarajan, S. Ambika, K. Bharathi, Plant-extract mediated synthesis of ZnO nanoparticles using *Pongamia pinnata* and their activity against pathogenic bacteria, Adv. Powder Technol. 26 (2015) 1294–1299.

[31] Nasrollahzadeh, M. Mehdi, S.M. Sajadi, Green synthesis of CuO nanoparticles by aqueous extract of Gundelia tournefortii and evaluation of their catalytic activity for the synthesis of N-monosubstituted ureas and reduction of 4-nitrophenol, J. Coll. Int. Sci. 455 (2015) 245–253.

[32] B. Halamoda-Kenzaoui, M. Ceridono, P. Urbán, A. Bogni, J. Ponti, S. Gioria, A. Kinsner-Ovaskainen, The agglomeration state of nanoparticles can influence the mechanism of their cellular internalization, J Nanobiotechnol. 15 (2017), https://doi.org/10.1186/s12951-017-0281-6.

[33] E. Alzahrani, Chitosan membrane embedded with ZnO/CuO nanocomposites for the photodegradation of fast green dye under artificial and solar irradiation, Anal. Chem. Insights 13 (2018) 1177390118763361.

[34] N. Zhou, L. Polavarapu, Q. Wang, Q.-H. Xu, Mesoporous SnO2-coated metal nanoparticles with enhanced catalytic efficiency, ACS Appl. Mater. Interfaces 7 (8) (2015) 4844–4850.

[35] C. Peng, C. Shen, S. Zheng, W. Yang, H. Hu, J. Liu, J. Shi, Transformation of CuO nanoparticles in the aquatic environment: influence of pH, electrolytes and natural organic matter, Nanomaterials (Basel) 7 (2017) 326, https://doi.org/10.3390/nano7100326.

[36] L. Wang, C. Hu, L. Shao, The antimicrobial activity of nanoparticles: present situation and prospects for the future, Int. J. Nanomed. 12 (2017) 1227–1249.

[37] M. Muniz-Miranda, C. Gellini, M. Pagliai, M. Innocenti, P.R. Salvi, V. Schettino, SERS and computational studies on microRNA chains adsorbed on silver surfaces, J. Phys. Chem. C 114 (2010) 13730–13735.

[38] A. Henglein, D. Meisel, Spectrophotometric observations of the adsorption of organosulfur compounds on colloidal silver nanoparticles, J. Phys. Chem. B 102 (1998) 8364–8366.

[39] X. Li, J.J. Lenhart, H.W. Walker, Dissolution-accompanied aggregation kinetics of silver nanoparticles, Langmuir 26 (2010) 16690–16698.

[40] J.Z. Guo, H. Cui, Lucigenin chemiluminescence induced by noble metal nanoparticles in the presence of adsorbates, J. Phys. Chem. C 111 (2007) 12254–12259.

[41] H.P. Wu, C.C. Huang, I.L. Cheng, W.L. Tseng, Sodium hydroxide as pretreatment and fluorosurfactant-capped gold nanoparticles as sensor for the highly selective detection of cysteine, Talanta 76 (2008) 347–352.

[42] J. Polte, Fundamental growth principles of colloidal metal nanoparticles – a new perspective, CrystEngComm. 17 (2015) 6809–6830.

[43] J.S. Lee, P.A. Ulmann, M.S. Han, C.A. Mirkin, A DNA-gold nanoparticle-based colorimetric competition assay for the detection of cysteine, Nano Lett. 8 (2008) 529–533.

[44] X. Wei, L. Qi, J. Tan, R. Liu, F. Wang, A colorimetric sensor for determination of cysteine by carboxymethyl cellulose-functionalized gold nanoparticles, Anal. Chim. Acta 671 (2010) 80–84.

[45] M. Zayats, S.P. Pogorelova, A.B. Kharitonov, O. Lioubashevski, E. Katz, I. Willner, Au nanoparticle-enhanced surface plasmon resonance sensing of biocatalytic transformations, Chem-A Europ. J. 9 (2003) 6108–6114.

[46] Y. Abboud, T. Saffaj, A. Chagraoui, A. El Bouari, K. Brouzi, O. Tanane, B. Ihssane, Biosynthesis, characterization and antimicrobial activity of copper oxide nanoparticles (CONPs) produced using brown alga extract (*Bifurcaria bifurcata*), Appl. Nanosci. 4 (2014) 571–576.

[47] A. Azam, A.S. Ahmed, M. Oves, M.S. Khan, S.S. Habib, A. Memic, Antimicrobial activity of metal oxide nanoparticles against Gram-positive and Gram-negative bacteria: a comparative study, Int. J. Nanomed. Nanosurg. 7 (2012) 6003–6009.

[48] K. Mageshwari, R. Sathyamoorthy, Flower-shaped CuO nanostructures: synthesis, characterization and antimicrobial activity, J. Mat. Sci. Technol. 29 (2013) 909–914.

[49] A. Sirelkhatim, S. Mahmud, A. Seeni, N.H.M. Kaus, L.C. Ann, S.K.M. Bakhori, H. Hasan, D. Mohamad, Review on zinc oxide nanoparticles: antibacterial activity and toxicity mechanism, Nano-micro Lett. 3 (2015) 219–242.

[50] Y.-N. Chang, M. Zhang, L. Xia, J. Zhang, G. Xing, The toxic effects and mechanisms of Cuo and Zno nanoparticles, Materials (Basel) 5 (2012) 2850–2871.

[51] S.E. Jin, W. Hwang, H.J. Lee, H.E. Jin, Dual UV irradiation-based metal oxide nanoparticles for enhanced antimicrobial activity in *Escherichia coli* and M13 bacteriophage, Int. J. Nanomed. Nanosurg. 12 (2017) 8057–8070.

[52] K.P. Raghupathi, R.T. Koodali, A.C. Manna, Size-dependentbacterial growth inhibition and mechanism of antibacterialactivity of zinc oxide nanoparticles, Langmuir 27 (2011) 4020–4028.

[53] H. Meruvu, M. Vangalapati, S.C. Chippada, S.R. Bammidi, Synthesis and characterization of zinc oxide nanoparticles and its antimicrobial activity against *Bacillus subtilis* and Escherichia coli, Rasayan J. Chem. 4 (2011) 217–222.

[54] M. Rautenberg, H.S. Joo, M. Otto, A. Peschel, Neutrophil responses to *Staphylococcal* pathogens and commensals via the formyl peptide receptor 2 relates to phenol-soluble modulin release and virulence, FASEB J. 25 (2011) 1254–1263.

[55] J. Matsui, K. Akamatsu, S. Nishiguchi, D. Miyoshi, H. Nawafune, K. Tamaki, N. Sugimoto, Composite of Au nanoparticles and molecularly imprinted polymer as a sensing material, Anal. Chem. 76 (2004) 1310–1315.

[56] J. Ramyadevi, K. Jeyasubramanian, A. Marikani, G. Rajakumar, A.A. Rahuman, Synthesis and antimicrobial activity of copper nanoparticles, Mater. Lett. 71 (2012) 114–116.

[57] Y.N. Slavin, J. Asnis, U.O. Häfeli, H. Bach, Metal nanoparticles: understanding the mechanisms behind antibacterial activity, J. Nanobiotechnol. 15 (2017) 65, https://doi.org/10.1186/s12951-017-0308-z.

[58] A. Lipovsky, Z. Tzitrinovich, H. Friedmann, G. Applerot, A. Gedanken, R. Lubart, EPR study of visible light-induced ROS generation by nanoparticles of ZnO, J. Phys. Chem. C 113 (2009) 15997–16001.

[59] P. Rajiv, S. Rajeshwari, R. Venckatesh, Rambutan peels promoted biomimetic synthesis of bioinspired zinc oxide nanochains for biomedical applications, Spectrochim, Acta Part A Mol. Biomol. Spectrosc. 112 (2013) 384–387.

[60] D. Klimm, Electronic materials with a wide band gap: recent developments, IUCrJ. 1 (2014) 281–290.

[61] Y. Kumar Mishra, G. Modi, V. Cretu, V. Postica, O. Lupan, T. Reimer, I. Paulowicz, V. Hrkac, W. Benecke, L. Kienle, R. Adelung, Direct growth of freestanding ZnO tetrapod networks for multifunctional applications in photocatalysis, uv photodetection, and gas sensing, ACS Appl. Mater. Interfaces 7 (2015) 14303–14316.

[62] I. Chanu, P. Krishnamurthi, P.T. Manoharan, Effect of silver on plasmonic, photocatalytic, and cytotoxicity of gold in auagzno nanocomposites, J. Phys. Chem. C 121 (2017) 9077–9088.

[63] A. Lipovsky, Z. Tzitrinovich, H. Friedmann, G. Applerot, A. Gedanken, R. Lubart, EPR study of visible light-induced ROS generation by nanoparticles of ZnO, J. Phys. Chem. C. 113 (2009) 15997–16001.

[64] L.-N. Ma, D.-J. Liu, Z.-X. Wang, Synthesis and applications of gold nanoparticle probes, Chinese J. Anal. Chem. 38 (2010) 1–7.